Research Article

Zeynep Betül Sari* and Tülin Çora

Tumor-endothelium reciprocal interactions in co-culture: changes of genetics and phenotypic characteristics of endothelial and laryngeal cells

https://doi.org/10.1515/tjb-2024-0187
Received August 2, 2024; accepted March 28, 2025;
published online May 23, 2025

Abstract

Objectives: This study aims to elucidate the interactions between laryngeal cancer cells (HEp-2) and endothelial cells (HUVEC) within the head and neck squamous cell cancer (HNSCC) microenvironment using direct and indirect *in vitro* co-cultivation systems.

Methods: Conditioned mediums (CM) of HEp-2 and HUVEC were generated, followed by the construction of co-culture systems. Confocal microscopy, XTT assay, trypan blue viability assay, real-time cell analysis system (RTCA), and quantitative real-time polymerase chain reaction (qRT-PCR) were used to assess cell morphology, proliferation, migration, invasion, and the expression of cancer-associated genes (*CDH2*, *CCL21*, *CXCL8*, *ITGB*, *MMP2*, *MMP9*, and *VIM*).

Results: We observed that the HEp2 co-culture effect altered HUVEC morphology, also reduced cell proliferation significantly, increased migration ($p<0.05$), and invasion of the cells. The mRNA levels of *CXCL8* and *ITGB* were downregulated significantly, while the expression level of *CCL21* mRNA was markedly upregulated (88.4-fold) compared to mono-culture HUVECs ($p<0.05$). Meanwhile, the HEp-2s showed a spindle-shaped and scattered morphology after co-culture with HUVEC. In addition, a higher relative migration rate ($p<0.05$) but significantly reduced proliferation and invasion rates of HEp2s were detected.

Conclusions: Reciprocal interactions between HEp2 and HUVEC significantly modulate cellular behaviors and gene expression, suggesting that these interactions play a crucial role in laryngeal cancer progression and offering potential insights for HNSCC treatment strategies.

Keywords: tumor microenvironment; co-culture system; head and neck squamous cell carcinoma; HEp2; HUVEC

Introduction

Cancer progression and initiation are strongly influenced by its microenvironment [1, 2]. Carcinogenesis is not considered a cancer cell-focused view. Tumor is the consequence of a complex, dynamic, and heterogeneous microenvironment [3–5]. The tumor microenvironment (TME) consists of cancer-associated fibroblasts (CAFs), endothelial cells (ECs), immune cells, blood and lymphatic tumor vessels, extracellular matrix (ECM), chemokines, and growth factors [6, 7]. In brief, it has been reported that the tumor microenvironment arises from the dynamic interplay between malignant and nonmalignant cells. TME is crucial in driving the proliferation, invasion, and metastasis of different cancers. It facilitates tumor survival, growth, angiogenesis, immune evasion, drug resistance, and the secretion of growth factors and cytokines [8, 9]. In addition, reciprocal interactions between tumor and stromal cells evolve as the tumor grows, which means the microenvironment interactions are bidirectional [10]. The stromal cells in tumor microenvironments gain abnormalities and show different properties from stromal cells in normal tissues; for example, Tumor-associated macrophages (TAMs) and CAFs differ from normal macrophages and fibroblasts, respectively [8, 11].

Laryngeal cancer, a subtype of head and neck squamous cell carcinoma (HNSCC), was chosen for study as the TME in this cancer type has been less studied compared to other cancers [12]. HNSCC ranks as the sixth most prevalent cancer type globally [13, 14]. Previously, the focus was primarily on aberrant genetic and epigenetic mutations in HNSCC. Now,

***Corresponding author: Zeynep Betül Sari**, Department of Medical Biology, Medical Faculty, Ankara Yıldırım Beyazıt University, Bilkent, Ankara, Türkiye, E-mail: zeynepbetulsari@aybu.edu.tr. https://orcid.org/0000-0003-0378-7673
Tülin Çora, Department of Medical Genetics, Medical Faculty, Selcuk University, Konya, Türkiye. https://orcid.org/0000-0001-9787-7519

investigating the tumor microenvironment is equally valuable, as various stromal components play a critical role in regulating HNSCC progression and metastasis. For this reason, interpreting the TME is crucial for analyzing, understanding, and managing cancer, as it can provide deeper insights into the mechanisms of HNSCC [3, 15]. Therefore, it is essential to develop new model systems that incorporate carcinoma cells along with tumor-associated endothelial cells to better understand the complex interactions in HNSCC. However, the precise roles of these cells within the tumor microenvironment of HNSCC remain unclear.

This study provides an opportunity to better understand the role of the tumor microenvironment in laryngeal cancer progression and its interactions with stromal components. Reports indicate that ECs directly support cancer progression via neoangiogenesis [16]. In addition, the effect of EC is not restricted to the making of blood vessels, but also the interaction between tumor and endothelial cells modifies the characteristics of tumor cells [17, 18]. Therefore, additional data is necessary to understand the impact of endothelial cells on the behavior of laryngeal cancer. To address this, we developed an *in vitro* co-culture system comprising human epithelial type 2 (HEp-2) cells and human umbilical vein endothelial cells (HUVEC). This system allowed us to simulate the cross-talk between HEp-2 and HUVEC cells and evaluate their effects on cell morphology, proliferation, migration, invasion, and gene expression.

Materials and methods

Cell culture and study designs

HUVEC cell line was supplied by Dr Timucin Avsar, and HEp-2 cell line was supplied by Dr Hasan Acar. HEp2 cells were transfected with a green fluorescent protein (GFP) to aid in the discrimination of the cells from HUVECs. GFP-HEp-2 cell line was obtained in the project of Hasan Acar et al. (TÜBİTAK-112S498). Both cell types were cultured in Dulbecco's modified eagle medium (DMEM, Gibco, USA) with 10 % fetal bovine serum (FBS, Gibco, USA) and 1 % penicillin/streptomycin (Gibco, USA) at 37 °C in a 5 % CO2 incubator. Stable GFP-expressing HEp-2 cells were expanded in growth media. For direct co-culture, HUVECs were grown to 80 % confluence for 24 h, and then GFP-HEp- two cells were added at a 4:1 ratio. Two types of indirect co-culture were performed. For the first type, which was used for the invasion assay, cells were cultured in 24-well Transwell chambers (Corning, USA) with or without Matrigel. The second type of indirect co-culture, used for proliferation, migration, and gene expression analyses, involved the use of conditioned medium (CM).

Preparation of the CM

HEp-2 and HUVEC cells were seeded into T75 culture flasks and cultured in DMEM for 30 h until reaching approximately 80 % confluence. The medium was then collected and centrifuged at 1,500 rpm for 5 min, and the supernatant was filtered to obtain CM for further studies. Various concentrations of CM, specifically 10 , 25, and 100 %, were prepared and utilized in experiments. For optimization, experiments were conducted with 100 % growth medium (cell control) and different CM concentrations (10 , 25, 50, and 100 %) in proliferation assays. Based on these results, 10 % CM was selected as the optimal concentration for subsequent experiments, including migration and gene expression analyses.

Morphology analysis

To evaluate the effect of co-culture on cell morphology, GFP-HEp-2 and HUVEC cell lines, both in mono-culture and direct co-culture, were examined daily for 120 h using an inverted laser scanning confocal microscope (Nikon A1R1, Japan). GFP was excited with a 488 nm laser line, and emission was detected at 510 nm.

Trypan blue staining

Cell viability was evaluated using a trypan blue exclusion assay. A total of 3×10^5 cells per well were seeded in a growth medium in 6-well plates. After overnight attachment and growth, control cells in mono-culture were fed with the growth medium, while co-culture cells were fed with 10 and 100 % CMs. Trypan blue staining was performed as previously described [19].

XTT proliferation assay

Cell growth rates in mono-cultures and co-cultures were determined by XTT assay. Cells were seeded into 96-well plates at a density of 5×10^3 per well. After overnight attachment and growth, mono-culture cells as control were fed with culture mediums, and the co-culture cells were fed with CMs of 10 and 25 %. Cell viability was assessed at 24, 48, and 72 h. The XTT kit (BI, USA) was used according to the

manufacturer's instructions. Results were obtained by detecting absorbance at a wavelength of 460 nm with the microplate reader (Biotek-Epoch, USA). The cell proliferation rate (%) was calculated using the formula (OD of sample/OD of control)×100. Three replicate wells were used for each analysis.

Real-time analysis of cell proliferation assay (RTCA)

Cell growth of mono-cultures and co-cultures of HEp-2 and HUVEC cells was continuously monitored using the xCELLigence RTCA MP instrument (ACEA Biosciences, USA). Briefly, cells were seeded into wells of E-plate View 16 (ACEA Biosciences, USA) at a density of 10^4/100 µL per well. After overnight attachment and growth, mono-culture cells as control were fed with growth mediums, and the co-culture cells were fed with CMs 10 and 100 % at the 25th hour, consistent with the XTT assay. RTCA assay was performed according to the previously published method [20]. The impedance was measured every 15 min for at least 120 h at 37 °C in a 5 % CO2 atmosphere. Cell proliferation rate was registered as an increase in the cell index (CI). All experiments were performed in duplicate. CI is a parameter used to monitor cell proliferation changes in real time. It is measured through electrical impedance-based systems like xCELLigence, reflecting cell density and attachment strength [21].

Wound healing and invasion assays

Cells in the growth medium were seeded in 24-well plates and were adhered to overnight (>90 % confluence). To suppress the proliferation of the cells, they were pretreated with mitomycin C (5 µg/mL) (Sigma, Germany) for 2 h. A wound-healing assay was subsequently performed to evaluate cell migration capacity. Photographs of the same area of the wound were taken at certain times (3, 6, 9, 12, 24, 48, 72 h) using a light inverted microscope (Leica, Germany). The migration distances were measured using Image J software (LOCI, USA) based on the images at time "0" as the reference point. To evaluate invasive capacity, a 24-well Transwell chamber invasion assay (Corning, USA) coated with Matrigel (Corning, USA) was used. Three fields (×100) were randomly selected for counting. The experiment is illustrated in Supplementary Material, Figure S1. Different co-culture systems were selected based on the requirements of each experiment: CM was used for migration, proliferation, and gene expression assays, while Transwell chambers were employed for invasion assays to provide a physical barrier that better simulates *in vivo* extracellular matrix interactions.

Quantitative real-time polymerase chain reaction (qRT-PCR)

For real-time PCR analysis, the HEp-2s and HUVECs were *in vitro* co-cultured for 24 h (short-term) and 21 days (long-term). Mono-culture HUVECs and mono-culture HEp-2s served as controls. Total RNA was extracted from the co-culture and mono-culture systems using the TRIzol reagent (Invitrogen, USA). For cDNA synthesis, 1 µg of total RNA from each pooled sample was reverse transcribed into cDNA using a 2-step RT-PCR kit (Vivantis, Malaysia) according to the manufacturer's instruction. cDNA was diluted 1:9 in sterile water. qPCR was performed on a Lightcycler 480 instrument (Roche, Light Cycle 480 II, Germany) using GoTaq® qPCR Master Mix (Promega, USA). The housekeeping gene *GAPDH* was used as the internal control for HEp-2s. The other housekeeping gene, *B2M,* was used as the internal control for HUVECs. The genes (*CDH2*, *CCL21*, *CXCL8*, *ITGB*, *MMP2*, *MMP9*, and *VIM*) were selected from those reported in the literature to be associated with cancer. The relative fold change in target gene expression was calculated using the comparative cycle threshold (2−ΔΔCT) method. All experiments were conducted in triplicate. Specific primers for PCR amplification were designed using IDT (http://eu.idtdna.com/home/home.aspx). The primers used are listed in Supplementary Material, Table S1.

Statistical analysis

Data were shown as mean + standard deviation (SD) from three independent experiments and analyzed using GraphPad Prism 6.00 (GraphPad Software, USA). Student's *t*-test was performed between groups for comparing treated and untreated cell groups. Statistical significance is indicated as *p<0.05, **p<0.01 ***p<0.001.

Results

Co-culture induces morphological changes in HEp-2 and HUVEC cells

To evaluate the direct co-culture effect on HEp-2 and HUVEC cell morphology, we examined the cells using confocal and

light microscopes. Control samples of HEp-2, grown separately, exhibited their characteristic rounded and connected morphology (Figure 1A–C). In contrast, after 120 h of co-culture, HEp-2 cells displayed a spindle-shaped morphology, becoming disjointed and scattered. Meanwhile, HUVECs in mono-culture appeared 'teardrop-like', but in co-culture, they developed net-like formations similar to a vascular network (Figure 1B–D).

Dose- and time-dependent effects of conditioned medium on cell proliferation

Treatment with 10 and 25 % HUVEC-CM significantly increased HEp-2 proliferation at 24 h by 1.6-fold and 1.5-fold, respectively ($p<0.001$ for both), but did not affect HEp-2 viability at 48 and 72 h (Figure 2A). Similarly, 10 % HEp2-CM treatment significantly increased HUVEC proliferation at 24

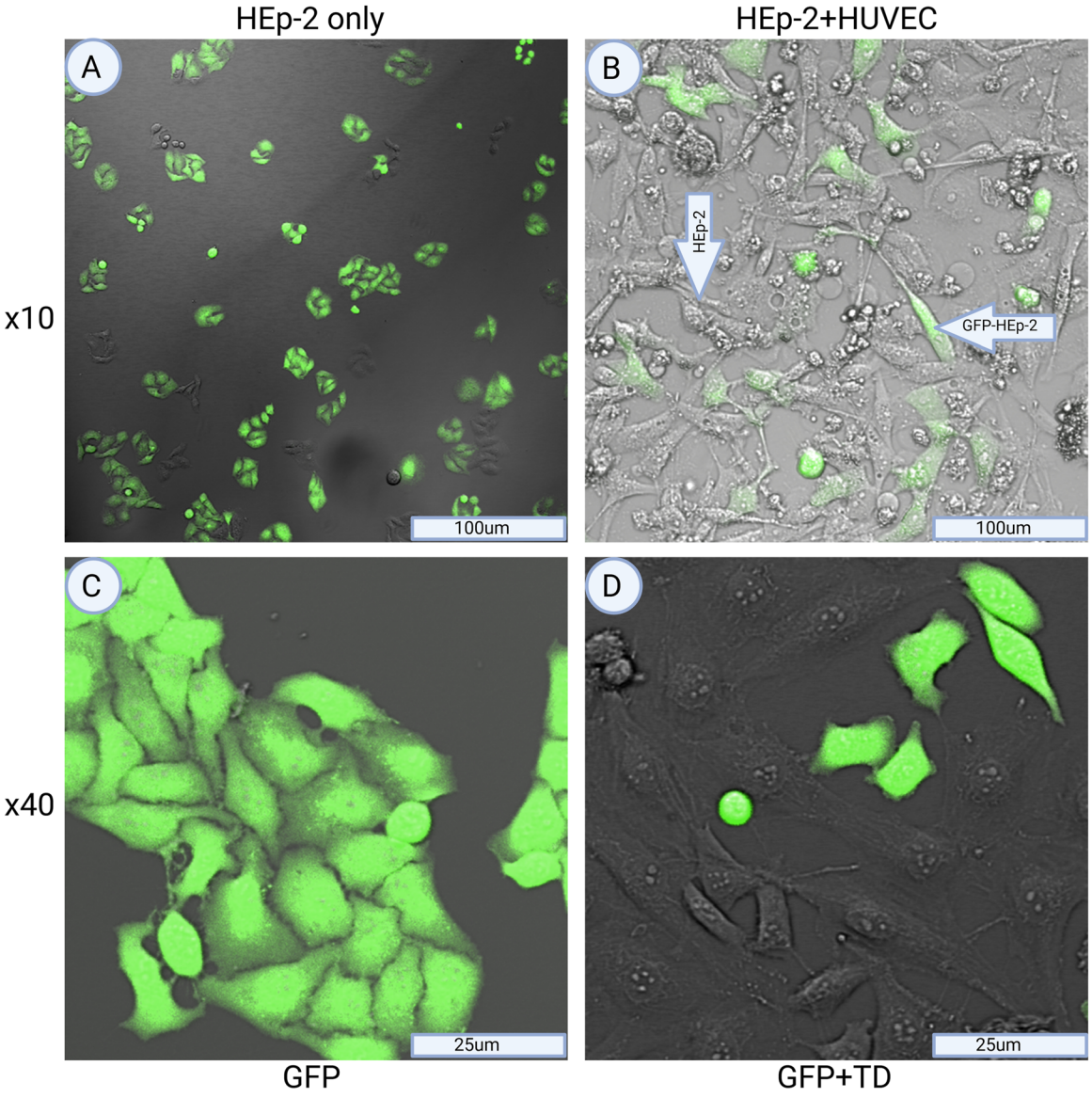

Figure 1: Confocal microscope images of GFP-HEp-2 and HUVEC cells at 10× and 40×magnification. Left panel mono-cultured GFP-HEp-2 cells in the GFP channel. Right panel co-cultured GFP- HEp-2 cells in GFP and TD merged channel. Co-cultured HEp-2 cells exhibited elongated shuttles (B, D), while monocultured HEp-2 cells maintained a rounded form (A, C). HUVECs formed net-like structures in co-culture (B). GFP, green fluorescence protein; TD, transmitted detector, bright field.

and 48 h by 1.5-fold and 1.3-fold, respectively (p=0.010 and p=0.002), with no significant changes in HUVEC viability at 72 h (Figure 2B). Cell proliferation was evaluated by cell counting, and it was found that 10 and 100 % HUVEC-CM significantly reduced HEp-2 cell numbers by 1.6-fold and 2.6-fold at 24 h (p=0.003 and p<0.001). At 72 h, the reduction was 1.6-fold and 3.2-fold, respectively (p=0.003 and p<0.001) (Figure 2C). These results indicate that HUVEC-conditioned medium inhibits HEp-2 cell proliferation in a dose and time-dependent manner. Additionally, Figure 2D demonstrates a significant reduction in HUVEC cell numbers following 24 h of treatment with 10 and 100 % HEp2-CM, showing reductions of 1.3-fold and 2.5-fold, respectively (p=0.026 and p<0.001). However, at 72 h, the number of HEp-2 cells treated with 100 % HUVEC-CM decreased much more significantly than the control cells, reaching up to a 32.8-fold reduction (p<0.001). These results underscore the substantial inhibitory effect of 100 % HUVEC-CM on HEp-2 cell proliferation over time.

In our study, discrepancies were observed between the results of the XTT assay and the trypan blue exclusion assay. While the XTT assay indicated that the CM increased cell proliferation at early time points, the trypan blue assay showed a reduction in cell numbers.

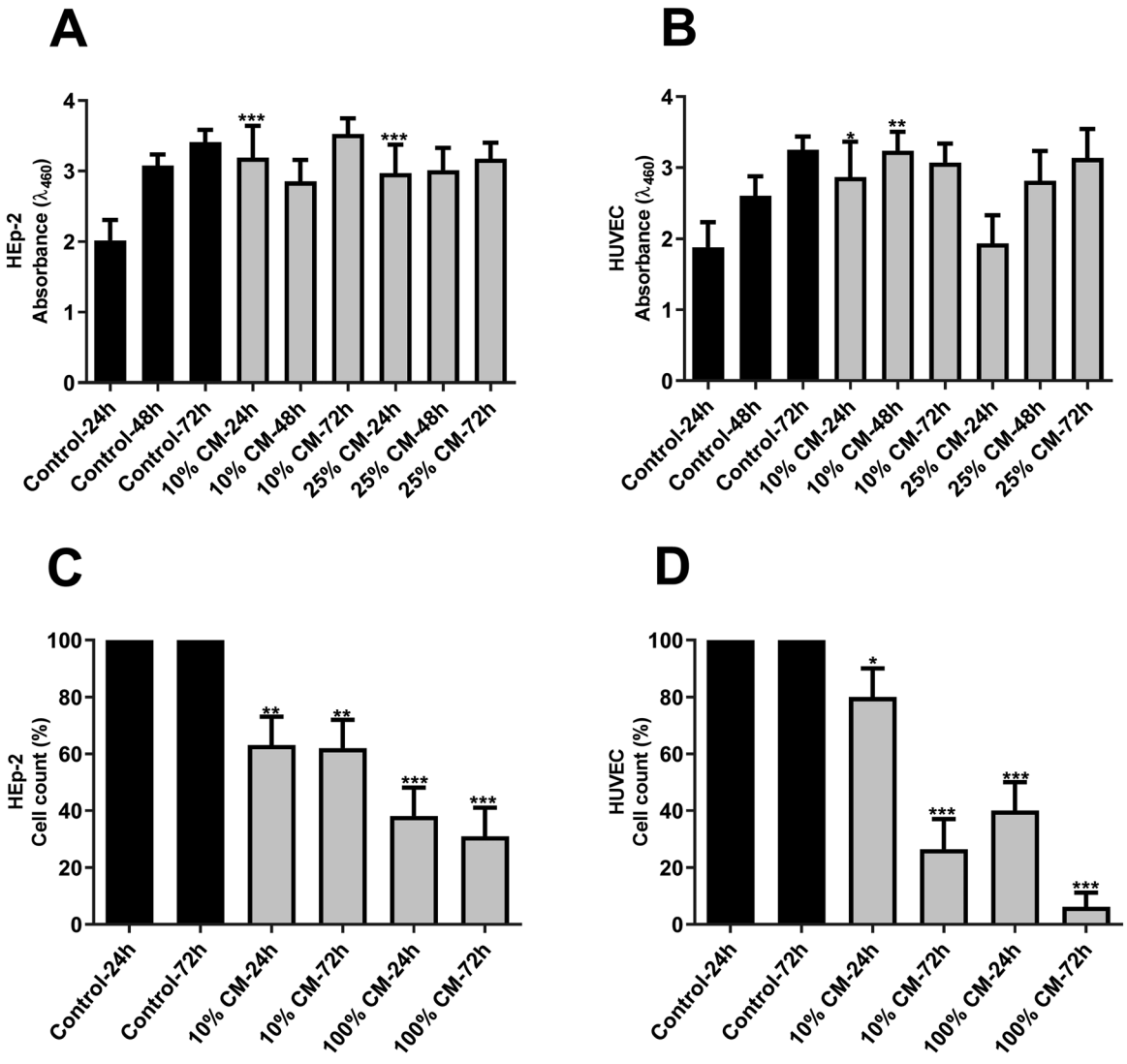

Figure 2: Effect of indirect co-culture on the cell viability of HEp-2 (A, C) and HUVEC (B, D). After HEp-2 and HUVEC cells treatment with DMEM 10 % FBS (control), HEp2-CM (10 %, 25 %), or HUVEC-CM (10 %, 25 %) for 24, 48, and 72 h, and XTT assay was performed to determine the viability of cells. HEp-2 (A) and HUVEC (B) in CM showed higher proliferation potentials than controls, depending on CM concentration and incubation time. After HEp-2 and HUVEC cells were treated with DMEM 10 % FBS (control), HEp2-CM, or HUVEC-CM for 24 and 72 h, cell proliferation was evaluated by trypan blue staining. The cell counts of HEp-2 (C) and HUVEC (D) were decreased significantly compared to that in the control mediums. *p<0.05, ** p<0.01, *** p<0.001. CM, conditioned medium.

Real-time monitoring of dynamic cell proliferation and attachment using the xCELLigence system

To assess the effects of CM on the proliferation and attachment of HEp-2 and HUVEC cells, the cells were monitored every 15 min for 120 h using the xCELLigence system. As illustrated in Figure 3A, the CI for each cell type, including controls, reached its peak at approximately 60 h after treatment with CM. Significant differences were observed between the HEp-2 control cells and those treated with 10 % CM, as well as between the HEp-2 control cells and those treated with 100 % CM ($p=0.012$ and $p<0.001$, respectively). Consequently, 10 and 100 % HUVEC-CM resulted in a 1.1-fold and 2.3-fold decrease in the HEp-2 CI (Figure 3B). In contrast, HUVEC cells showed minimal response to CM treatment, with cell indices nearly identical between the control and treated groups. No significant differences were

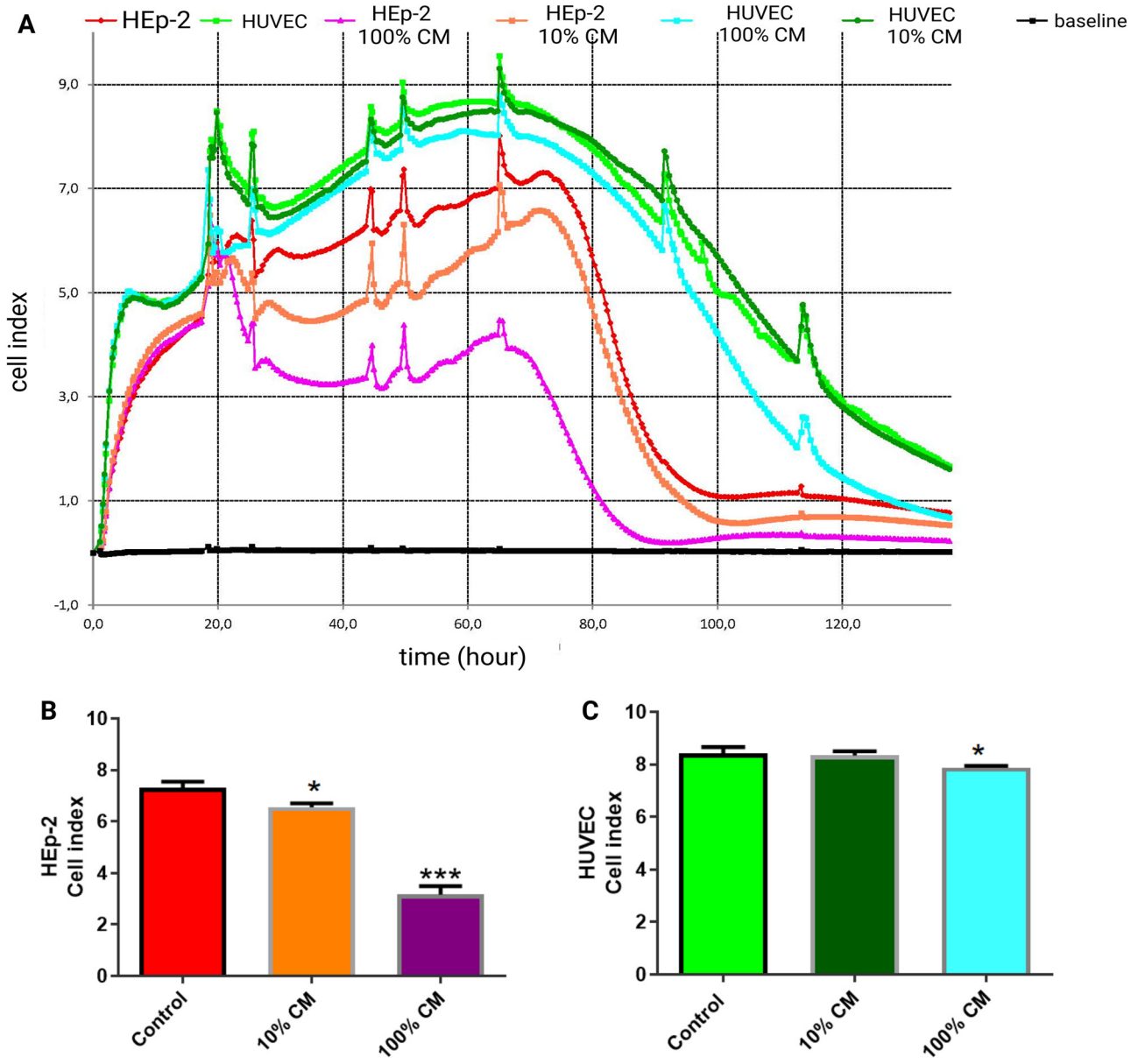

Figure 3: Effects of conditioned medium on HEp-2 and HUVEC cell index: Time-dependent analysis and quantification. Effects of 10 and 100 % CM during 120 h exposure on the viability of HEp-2 and HUVECs were measured based on the cell index by the xCELLigence system. (A) The cell index plot of HEp-2 (red line), HUVEC (light green line), HEp-2-100 % CM (purple line), HEp-2-10 % CM (orange line), HUVEC-100 % CM (blue line), HUVEC-10 % CM (dark green), baseline (black line). The bar diagram represents the cell index of HEp-2 (B) and HUVEC (C) in various percentage concentrations of HEp-2-CM and the HUVEC-CM models. *p<0.05, *** p<0.001. CM, conditioned medium.

observed in the HUVEC control cells and those treated with 10 % CM. However, treatment with 100 % HEp2-CM significantly reduced HUVEC proliferation (p=0.013) (Figure 3C).

Enhanced wound healing capacity of HEp-2 and HUVEC cells induced by CMs

Whether CMs induce cell migration in HEp-2 and HUVEC cells was investigated using a gap closure assay to measure differences in migration capacities. By the 24th h, co-cultured HEp-2 cells had completely closed the gaps, while co-cultured HUVEC cells achieved complete gap closure by the 48th h. The wound-healing rates were significantly higher in both HEp-2 and HUVEC cells treated with CM, showing 2.3-fold and 3-fold increases, respectively, compared to cells grown in serum-free medium (p=0.013 and p=0.030) (Figure 4A and B). The light microscope images of HEp-2 and HUVEC migration were consistent with the results (Figure 4C and D). These findings suggest that both HEp-2-CM and HUVEC-CM significantly promote the migration capacity of HEp-2 and HUVEC cells.

Decreased invasion capacity of HEp-2 cells induced by co-culture with HUVECs

Fewer HEp-2 cells co-cultured with HUVECs were seen invading across the Matrigel compared to the control cells. This suggests that co-cultured HUVECs reduced the invasion potential of HEp-2 cells by approximately 2-fold (p=0.049) (Figure 4E). Conversely, HUVECs co-cultured with HEp-2 cells did not exhibit a significantly higher invasion capacity compared to HUVECs cultured alone (p=0.287) (Figure 5F). The light microscope images of HEp-2 and HUVEC invasion were consistent with the results (Figure 4G and H).

Gene expression patterns of HEp-2 and HUVEC cells treated with HUVEC CM or HEp- 2 CM

Changes in proliferation, migration, and invasion in HEp-2 and HUVEC cells treated with CM or in co-culture were observed, leading to the investigation of the underlying molecular mechanisms. Accordingly, the mRNA expression levels of genes significantly associated with cancer prognosis were evaluated. The mRNA levels of *CDH2*, *CCL21*, *CXCL8*, *ITGB*, *MMP2*, *MMP9*, and *VIM* genes were significantly downregulated in HEp-2 cells grown in co-culture, with expression levels reduced by up to 0.05-fold at either 24 h or 21 days (Figure 5). Similarly, the mRNA levels of *CXCL8* and *ITGB* were significantly downregulated in HUVEC cells grown in co-culture at 24 h or 21 days (Figure 5C and D). Meanwhile, a significant increase in the expression level of *CCL21* mRNA (88.4-fold) was detected in HUVEC cells at 21 days (p=0.039) (Figure 5B).

Discussion

Cancer is a multifactorial and dynamic disease, presenting significant challenges in terms of treatment. Additionally, tumor microenvironments exhibit considerable heterogeneity in both cellular composition and ECM structure [22]. In this study, co-culture platforms were presented to help highlight tumor biology, addressing the need for the development of *in vitro* models that mimic the *in vivo* environment.

The microenvironment interactions are bidirectional. Reciprocal cross-talking between tumor and endothelial cells develops and differentiates as the tumor grows [23]. Therefore, in this study, the investigation was not limited to tumor-cell-induced changes in EC or healthy-cell-induced changes in tumor cells. ECs in a tumor microenvironment induce or reduce the aggressive behavior of tumor cells [24]. In parallel, tumor cells may have two-edged effects on endothelial cells [25]. To date, to our knowledge, the effects of ECs on HNSCC and vice versa are not apparent. In this study, it was hypothesized that, under *in vitro* co-culture conditions, laryngeal carcinoma cells would induce aggressiveness in endothelial cells, while endothelial cells would reduce the aggressiveness of tumor cells. To evaluate the influence of the microenvironment on cells in the co-culture, a healthy cell line, HUVEC, and a cancer cell line, HEp-2, were selected to study the morphological, cellular, and molecular changes caused by this interaction. It was shown through our analysis that co-cultured GFP-HEp-2s exhibited spindle-shaped and scattered morphology. They also exhibited elongated protrusions, indicating invasion potential. But interestingly, in the indirect co-culture, the invasion rate of HEp-2 decreased. It can be speculated that proteases are suppressed in the microenvironment of HUVEC cells. The obtained results are consistent with the data reported by Li et al., who established a co-culture study with a lung cancer cell line (A549). Co-cultured A549 cells showed a more scattered and spindle-shaped morphology [26]. This situation led us to believe that similar morphological changes may be related to the epithelial origin of A549 and HEp-2 cells.

On the other hand, in this study, it was also demonstrated that structures resembling a vascular network were

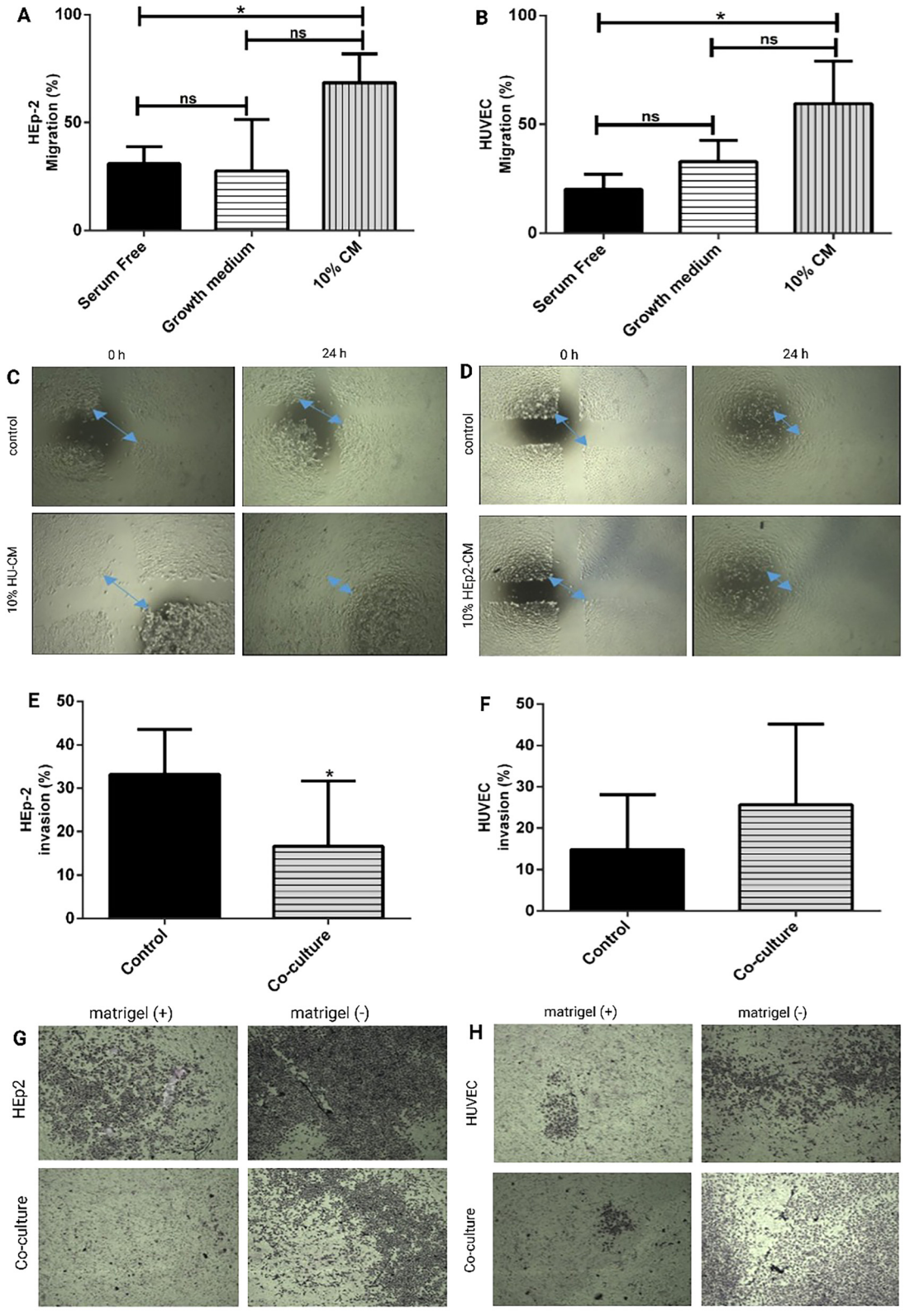

Figure 4: Effects of conditioned medium and co-culture on migration and invasion of HEp-2 and HUVEC cells. (A) Migration of HEp-2 cells under three different conditions: Serum-free medium, growth medium, and 10 % HUVEC-CM, evaluated over 24 h (B) Migration of HUVEC cells under three different conditions: Serum-free medium, growth medium, and 10 % HEp-2-CM, evaluated over 24 h. the percentage of migration was calculated based on the wound-healing assay. (C) Representative images of HEp-2 cell migration at 0 and 24 h under control (growth medium) and 10 % HUVEC-CM conditions.
(D) representative images of HUVEC cell migration at 0 and 24 h under control (growth medium) and 10 % HEp-2-CM conditions. Blue arrows indicate the wound area. The spreading speeds of HEp-2 (A) and HUVEC (B) cells in 10 % CM along the wound edge were faster than those in controls. Comparison of the

developed by co-cultured HUVECs, but mono-cultured HUVECs were observed as 'teardrop-like'. Consistent with our morphological data, Khodarev et al. [27] reported co-cultivation of HUVECs with U87 (glioma cells) formed net-like structures. Considering these results, it can be concluded that this kind of organization in these cells indicates a morphological rearrangement of the co-culture system due to modifications in the microenvironment.

Furthermore, our morphological observations under the light microscope revealed that in direct co-culture, HUVEC suppressed HEp-2 proliferation, likely due to high levels of apoptotic and antimitogenic proteins in the medium. However, under indirect co-culture conditions using CM, results varied with different proliferation assays. The XTT assay indicated increased HEp-2 proliferation, whereas the trypan blue and RTCA assays showed decreased proliferation. These discrepancies may be attributed to the differing sensitivities and natures of the tests, with RTCA being more capable of detecting sensitive growth inhibitory factors. While the nuclear counting method is regarded as the most precise for assessing cell viability [28], but the ease of applying metabolic-based assays such as MTT/XTT enables widespread use [29]. These assays depend on tetrazolium salt reduction to formazan, which reflects changes in the metabolic state rather than absolute cell viability. Studies such as those by Stockert et al. [30] and Riss et al. [31] have highlighted that factors like oxidative stress and energy demands can influence these results, potentially causing discrepancies with other methods. In our study, such differences may arise from variations in mitochondrial activity under specific conditions. While XTT offers valuable insights, complementary techniques, like flow cytometry or live/dead staining, are recommended for a more complete assessment.

Stromal cells are crucial in cancer progression, growth, and spread [32]. If the migration and invasion capacities of cells increase, their proliferation capacity must also increase [33]. Neiva reported that the proliferation rates of co-cultured HNSCC cells with endothelial cell line HDMEC cells did not alter, but migration rates increased [18]. We found that HUVEC- CM increased the proliferation rates of HEp2 cells (depending on the test used) and migration rates of cancer cells but suppressed its invasion. Thus, variations in experimental conditions, such as the kinds of cell lines and direct or indirect co-cultures, affect the results [34]. Specifically, for HEp-2 cells, the use of 100 % CM could potentially mask or exaggerate the effects of secreted factors, leading to a misinterpretation of proliferation results. Similarly, for HUVEC cells treated with 100 % CM, we recognize that the results obtained via xCELLigence could be influenced by toxic components in the medium.

The intricate interactions between tumor and endothelial cells, resembling those in embryonic development, are vital for tumor angiogenesis [35]. In another co-culture study, U87 human glioma cells were co-cultured with HUVEC to investigate tumor/endothelial cell interactions [27]. U87 cells have been shown to enhance proliferation and migration in HUVECs. Signals originating from tumor cells play an important role in the activation of normal fibroblasts (NFs) to CAFs. Moreover, NFs can be converted to CAFs by co-culture with cancer cells [36]. Based on this data, it was predicted that co-cultured HUVEC might also transform into tumor-associated endothelial cells. Our proliferation, migration, invasion, and some gene expression results of co-cultured HUVEC supported this hypothesis. Accordingly, the HEp-2 microenvironment may contain biofactors that increase HUVEC adhesion kinetics and migration.

Analysis of gene expression profiles highlights altered ECM and tumor progression, invasion, and metastasis, emphasizing the significance of changes in gene expression levels in co-cultures [37]. Elevated N-cadherin (*CDH2* gene) expression is linked to epithelial-mesenchymal transition (EMT) in cancer [35]. In our study, N-cadherin levels significantly decreased in both HUVEC and HEp-2 cells ($p<0.05$). This suggests that the co-culture environment did not induce mesenchymal transition in these cells, although determining EMT status cannot rely on a single marker.

CCL21 overexpression has been found to be associated with the proliferation, progression, and metastasis of cancer cells [38]. In our study, the gene *CCL21* expression of HUVEC was dramatically altered under co-culture conditions ($p<0.05$). This finding is consistent with the proliferation, migration, and invasion findings of HUVEC. Conversely, HUVEC-CM caused a significant decrease in *CCL21* expression in HEp-2 cells ($p<0.05$). This finding is consistent with the proliferation and invasion findings of HEp-2.

CXCL8 (IL-8) plays a crucial role in promoting tumor cell proliferation, angiogenesis, tissue invasion, and metastatic spread through autocrine and paracrine signaling pathways while also contributing to inflammation and tumor

invasion percentage of HEp-2 (E) and HUVEC (F) cells under control conditions and co-culture conditions. Matrigel invasion assay results show a statistically significant reduction in HEp-2 cell invasion in the co-culture group compared to the control group ($p=0.049$). Representative images of HEp-2 (G) and HUVEC (H) cell invasion through Matrigel (Matrigel +) and without Matrigel (Matrigel -) under control and co-culture conditions. Matrigel (+) images depict cells that successfully invaded through the Matrigel layer, while Matrigel (–) images show non-specific migration. Similar to HEp-2 cells, Matrigel (+) and Matrigel (–) images demonstrate the invasion and migration ability of HUVEC cells in both conditions. *$p<0.05$. CM, conditioned medium; ns, not significant.

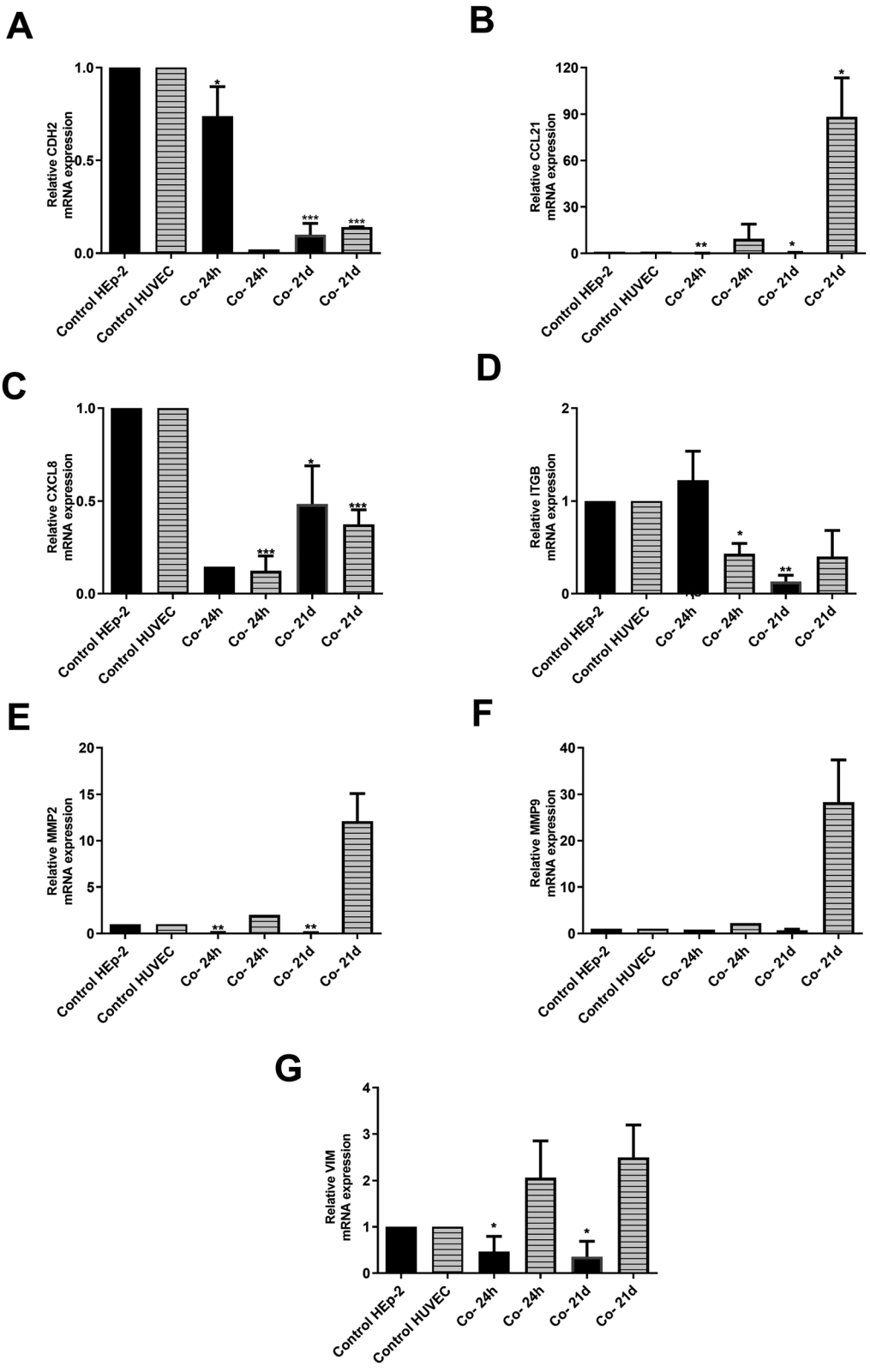

Figure 5: Gene expression profiles of HEp-2 and HUVEC cells treated with HUVEC CM or HEp-2 CM. qRT-PCR of *CDH2* (A), *CLC21* (B), *CXCL8* (C), *ITGB* (D), *MMP2* (E), *MMP9* (F) and *VIM* (G) genes in co-cultured HEp-2 and HUVEC cells treated with corresponding CM for 24 h or 21 days. The expression level of *CCL21* mRNA (B) was markedly increased (88.4-fold) in HUVEC cells when treated with HEp2-CM at 21 days. *p<0.05, **p<0.01, ***p<0.001. CM, conditioned medium; Co-24 h, co-culture condition after 24 h; Co-21 d, co-culture condition after 21 days.

progression [34]. But, IL-8 gene expression significantly decreased ($p<0.05$) in both endothelial cells co-cultured with HEp-2 and tumor cells co-cultured with HUVEC, with HEp-2-CM reducing IL-8 expression despite its promigratory and pro-invasive effects, aligning with RTCA analysis findings.

ITGB1, critical for tumor initiation, progression, and metastasis [39], showed a significant decrease in expression in HUVECs exposed to HEp-2-CM ($p<0.05$) and in HEp-2 cells exposed to HUVEC-CM during long-term co-culture ($p<0.001$). However, no significant change in *ITGB1* expression was observed in short-term co-culture.

MMP2 and *MMP9* are overexpressed in various malignant cancers and are also frequently linked to tumor grade and poor patient prognosis [40]. Among MMPs, *MMP2* and *MMP9* have well-characterized roles in the invasion and metastasis of cancer cells [41]. The gene showing the greatest up-regulation in HUVECs when co-cultured with HEp-2s was *MMP2* and *MMP9,* which is consistent with increased invasiveness in co-culture in our study ($p<0.05$). Conversely, HUVEC-CM condition caused a significant decrease in *MMP2* and *MMP9* expressions in HEp-2 cells. This finding is consistent with decreased *MMP2* and *MMP9* expression of HEp-2 cells with reduced invasiveness in co-culture.

VIM, a key EMT marker [42], was upregulated in HUVECs treated with HEp-2-CM, while *CDH2* (N-cadherin) was downregulated. However, the absence of simultaneous upregulation of EMT markers weakens the conclusion that HEp-2-CM induces EMT in HUVECs.

In conclusion, this experimental study may provide useful data for further comprehensive analyses of the reciprocal and critical interactions between laryngeal cancer and endothelial cells, which contribute to cancer progression. In addition, our further studies will focus on studying more genes relevant to head and neck cancer progression, and the results should also be validated at the protein levels. To mimic the tumor microenvironment at a better level, co-cultures should also include mesenchymal stem cells, TAMs, or CAFs in the HNSCC microenvironment.

Acknowledgments: We would like to thank Dr. Hasan Acar for the Hep-2 cells and Dr. Timuçin Avşar for the HUVEC cells used in this study. We are grateful to Dr. Emine YAVUZ for the helpful discussions on this manuscript. The authors also thank Muhammed Emin Sarı for his technical assistance.

Research ethics: Ethical Approval for the cell culture study was received from the Committee of Selcuk University Medical Faculty (Ethical Approval no:2017/212, dated July 26, 2017).

Informed consent: Not applicable.

Author contributions: All authors have accepted responsibility for the entire content of this manuscript and approved its submission.

Use of Large Language Models, AI and Machine Learning Tools: None declared.

Conflict of interest: Authors state no conflict of interest.

Research funding: This research was supported by Selcuk University Scientific Research Projects Coordinatorship with project number 17102029.

Data availability: The raw data can be obtained on request from the corresponding author.

References

1. Kucerova L, Skolekova S. Tumor microenvironment and the role of mesenchymal stromal cells. Neoplasma 2013;60:1–10.
2. Binnewies M, Roberts EW, Kersten K, Chan V, Fearon DF, Merad M, et al. Understanding the tumor immune microenvironment (TIME) for effective therapy. Nat Med 2018;24:541–50.
3. Peltanova B, Raudenska M, Masarik M. Effect of tumor microenvironment on pathogenesis of the head and neck squamous cell carcinoma: a systematic review. Mol Cancer 2019;18:63.
4. Yoon NK, Maresh EL, Shen D, Elshimali Y, Apple S, Horvath S, et al. Higher levels of GATA3 predict better survival in women with breast cancer. Hum Pathol 2010;41:1794–801.
5. Bissell MJ, Hines WC. Why don't we get more cancer? A proposed role of the microenvironment in restraining cancer progression. Nat Med 2011;17:320–9.
6. Feig C, Gopinathan A, Neesse A, Chan DS, Cook N, Tuveson DA. The pancreas cancer microenvironment. Clin Cancer Res 2012;18:4266–76.
7. Xiong Y, McDonald LT, Russell DL, Kelly RR, Wilson KR, Mehrotra M, et al. Hematopoietic stem cell-derived adipocytes and fibroblasts in the tumor microenvironment. World J Stem Cell 2015;7:253–65.
8. Kalluri R, Zeisberg M. Fibroblasts in cancer. Nat Rev Cancer 2006;6: 392–401.
9. Hanahan D, Coussens LM. Accessories to the crime: functions of cells recruited to the tumor microenvironment. Cancer Cell 2012;21:309–22.
10. Rodrigues-Lisoni FC, Peitl P Jr., Vidotto A, Polachini GM, Maniglia JV, Carmona-Raphe J, et al. Genomics and proteomics approaches to the study of cancer-stroma interactions. BMC Med Genom 2010;3:14.
11. Midgley AC, Rogers M, Hallett MB, Clayton A, Bowen T, Phillips AO, et al. Transforming growth factor-β1 (TGF-β1)-stimulated fibroblast to myofibroblast differentiation is mediated by hyaluronan (HA)-facilitated epidermal growth factor receptor (EGFR) and CD44 co-localization in lipid rafts. J Biol Chem 2013;288:14824–38.
12. Tudor F, Marijić B, Babarović E, Hadžisejdić I. Significance of PD-L1 and tumor microenvironment in laryngeal squamous cell cancer. Cancers (Basel) 2024;16:2645.
13. Sung H, Ferlay J, Siegel RL, Laversanne M, Soerjomataram I, Jemal A, et al. Global cancer statistics 2020: GLOBOCAN estimates of incidence and mortality worldwide for 36 cancers in 185 countries. CA Cancer J Clin 2021;71:209–49.
14. Bray F, Ferlay J, Soerjomataram I, Siegel RL, Torre LA, Jemal A. Global cancer statistics 2018: GLOBOCAN estimates of incidence and mortality worldwide for 36 cancers in 185 countries. CA Cancer J Clin 2018;68: 394–424.

15. Korneev KV, Atretkhany KN, Drutskaya MS, Grivennikov SI, Kuprash DV, Nedospasov SA. TLR-signaling and proinflammatory cytokines as drivers of tumorigenesis. Cytokine 2017;89:127–35.
16. Ding T, Xu J, Zhang Y, Guo RP, Wu WC, Zhang SD, et al. Endothelium-coated tumor clusters are associated with poor prognosis and micrometastasis of hepatocellular carcinoma after resection. Cancer 2011;117:4878–89.
17. Manzi M, Bacigalupo ML, Carabias P, Elola MT, Wolfenstein-Todel C, Rabinovich GA, et al. Galectin-1 controls the proliferation and migration of liver sinusoidal endothelial cells and their interaction with hepatocarcinoma cells. J Cell Physiol 2016;231:1522–33.
18. Neiva KG, Warner KA, Campos MS, Zhang Z, Moren J, Danciu TE, et al. Endothelial cell-derived interleukin-6 regulates tumor growth. BMC Cancer 2014;14:99.
19. Acar MS, Bulut ZB, Ateş A, Nami B, Koçak N, Yıldız B. Titanium dioxide nanoparticles induce cytotoxicity and reduce mitotic index in human amniotic fluid-derived cells. Hum Exp Toxicol 2015;34:74–82.
20. Ülker M, Çelik ACT, Yavuz E, Kahvecioğlu F, Ülker HE. Real-time analysis of antiproliferative effects of mouthwashes containing alcohol, sodium fluoride, cetylpyridinium chloride, and chlorhexidine in vitro. BioMed Res Int 2021;2021:2610122.
21. Teng Z, Kuang X, Wang J, Zhang X. Real-time cell analysis–a new method for dynamic, quantitative measurement of infectious viruses and antiserum neutralizing activity. J Virol Methods 2013;193:364–70.
22. Hanahan D, Weinberg RA. Hallmarks of cancer: the next generation. Cell 2011;144:646–74.
23. de Miranda MC, Melo MIA, Cunha PDS, Gentilini JJ, Faria J, Rodrigues MA, et al. Roles of mesenchymal stromal cells in the head and neck cancer microenvironment. Biomed Pharmacother 2021;144:112269.
24. Leone P, Malerba E, Susca N, Favoino E, Perosa F, Brunori G, et al. Endothelial cells in tumor microenvironment: insights and perspectives. Front Immunol 2024;15:1367875.
25. Wei C, Tang M, Xu Z, Yang L, Lv Y. Role of endothelial cells in the regulation of mechanical microenvironment on tumor progression. Acta Mech Sin 2021;37:218–28.
26. Li X, Tai HH. Activation of thromboxane A2 receptor (TP) increases the expression of monocyte chemoattractant protein -1 (MCP-1)/chemokine (C-C motif) ligand 2 (CCL2) and recruits macrophages to promote invasion of lung cancer cells. PLoS One 2013;8:e54073.
27. Khodarev NN, Yu J, Labay E, Darga T, Brown CK, Mauceri HJ, et al. Tumour-endothelium interactions in co-culture: coordinated changes of gene expression profiles and phenotypic properties of endothelial cells. J Cell Sci 2003;116:1013–22.
28. Chan GK, Kleinheinz TL, Peterson D, Moffat JG. A simple high-content cell cycle assay reveals frequent discrepancies between cell number and ATP and MTS proliferation assays. PLoS One 2013;8:e63583.
29. Single A, Beetham H, Telford BJ, Guilford P, Chen A. A comparison of real-time and endpoint cell viability assays for improved synthetic lethal drug validation. J Biomol Screen 2015;20:1286–93.
30. Stockert JC, Horobin RW, Colombo LL, Blázquez-Castro A. Tetrazolium salts and formazan products in Cell Biology: viability assessment, fluorescence imaging, and labeling perspectives. Acta Histochem 2018;120:159–67.
31. Riss TL, Moravec RA, Niles AL, Duellman S, Benink HA, Worzella TJ, et al. Cell viability assays. In: Markossian S, Grossman A, Baskir H, editors. Assay Guidance Manual [Internet]. Bethesda (MD): Eli Lilly & Company and the National Center for Advancing Translational Sciences; 2016.
32. Bremnes RM, Dønnem T, Al-Saad S, Al-Shibli K, Andersen S, Sirera R, et al. The role of tumor stroma in cancer progression and prognosis: emphasis on carcinoma-associated fibroblasts and non-small cell lung cancer. J Thorac Oncol 2011;6:209–17.
33. Ding Q, Xia Y, Ding S, Lu P, Sun L, Fan Y, et al. Potential role of CXCL9 induced by endothelial cells/CD133+ liver cancer cells co-culture system in tumor transendothelial migration. Genes Cancer 2016;7:254–9.
34. Iacopino F, Angelucci C, Sica G. Interactions between normal human fibroblasts and human prostate cancer cells in a co-culture system. Anticancer Res 2012;32:1579–88.
35. Darland DC, D'Amore PA. Blood vessel maturation: vascular development comes of age. J Clin Investig 1999;103:157–8.
36. Erez N, Glanz S, Raz Y, Avivi C, Barshack I. Cancer associated fibroblasts express pro-inflammatory factors in human breast and ovarian tumors. Biochem Biophys Res Commun 2013;437:397–402.
37. Gallagher PG, Bao Y, Prorock A, Zigrino P, Nischt R, Politi V, et al. Gene expression profiling reveals cross-talk between melanoma and fibroblasts: implications for host-tumor interactions in metastasis. Cancer Res 2005;65:4134–46.
38. Xu Y, Liu L, Qiu X, Jiang L, Huang B, Li H, et al. CCL21/CCR7 promotes G2/M phase progression via the ERK pathway in human non-small cell lung cancer cells. PLoS One 2011;6:e21119.
39. Kaplan-Türköz B, Jiménez-Soto LF, Dian C, Ertl C, Remaut H, Louche A, et al. Structural insights into Helicobacter pylori oncoprotein CagA interaction with β1 integrin. Proc Natl Acad Sci USA 2012;109:14640–5.
40. Uloza V, Liutkevičius V, Pangonytė D, Saferis V, Lesauskaitė V. Expression of matrix metalloproteinases (MMP-2 and MMP-9) in recurrent respiratory papillomas and laryngeal carcinoma: clinical and morphological parallels. Eur Arch Otorhinolaryngol 2011;268:871–8.
41. Roh MR, Zheng Z, Kim HS, Kwon JE, Jeung HC, Rha SY, et al. Differential expression patterns of MMPs and their role in the invasion of epithelial premalignant tumors and invasive cutaneous squamous cell carcinoma. Exp Mol Pathol 2012;92:236–42.
42. Thiery JP, Sleeman JP. Complex networks orchestrate epithelial-mesenchymal transitions. Nat Rev Mol Cell Biol 2006;7:131–42.

Supplementary Material: This article contains supplementary material (https://doi.org/10.1515/tjb-2024-0187).